IHJPAS. 37 (1) 2024
Ibn Al-Haitham Journal for Pure and Applied Sciences
Journal homepage: jih.uobaghdad.edu.iq
PISSN: 1609-4042, EISSN: 2521-3407

Fast New Method for Estimation of Captopril in Pure and Pharmaceutical Preparation by Reaction with Ammonium Ce (IV) Sulfate in Acid Medium

[1]Muntadhar Mohammed Jabbar* **[2]Elham Nghaimesh Mezaal**
[1,2]Department of chemistry, College of Education for Pure Science Ibn Al-Haitham, University of Baghdad, Baghdad, Iraq.

*Corresponding Author: muntadhar.jabbar2105m@ihcoedu.uobaghdad.edu.iq

Received 16 January 2023, Received 20 February 2023, Accepted 27 February 2023, Published 20 January 2024

doi.org/10.30526/37.1.3191

Abstract

The determination of captopril (CAP) using a new continuous flow injection analysis (CFIA) method was given in this work CAP in its pure state and some of its pharmaceutical preparations. The technique can be described as simple, fast, sensitive, easy to operate, and low-cost. The CAP reacted with ammonium ceric(IV) sulfate (ACS)2$(NH_4)_2SO_4Ce(SO_4)_2$. $3\frac{1}{2}H_2O$ in an acidic medium and the reaction led to the formation of a white, slightly yellowish precipitate. The formed precipitate was studied using Ayah 6S×1-ST-2D Solar cell-CFI Analyzer, a through the reflection of accident light on the surfaces of the precipitate particles at $(0\text{-}180^0)$, expressed as the response of the transducer measured in (mV). Some chemical and physical parameters were studied to provide the optimal conditions for the study. The calibration curve within the range of (0.07-3.0) mmol/L was linear, with a correlation coefficient (r) value equal to (0.9983), and the percentage value of linearity (R2%) was (99.65). The method's detection limit (L.O.D.) of the new method was 272.5 ng/25 µL; it was calculated by diluting the minimum concentration in the calibration curve gradually. RSD% was less than 0.2% for 0.9, 1.5, and 3.0 mmol/L concentrations of C.A.P. for n=8. The method was successfully applied to estimate C.A.P. in three pharmaceutical preparations, each produced by a different company. The new method was compared with the UV-Spectrophotometric method (classical method) at λmax= 207.2 nm by using the method of standard additions. Both the t-test and the F-test were conducted to ensure that there wasn't a significant difference between the new method and the conventional one. The results of both tests showed, at a confidence level of 95%, that there was no significant difference.

Keywords: Captopril, Flow injection analysis, Hypertension, Ayah 6S×1-ST-2D solar cell Continuous flow injection analyzer.

1. Introduction

Arterial hypertension is one of the most prevalent diseases in the world [1,2] due to many factors, including those related to old age, family medical history, weight gain, stress, psychological stress, excessive salt intake, excessive drinking of alcohol, smoking In addition to other reasons [3,4]. This necessitated the search for effective medications to treat this disease; the first controlled therapy used in the treatment of arterial hypertension was captopril [5]. Pure captopril appears as a white crystalline powder with a slight sulfur odor [6], chemically named-[(2S)-3-mercapto-2-methylpropionyl]-L-proline [7,8], its chemical formula $C_9H_{15}NO_3S$ (M.Wt=217.29 g/mol), the molecular structure of CAP is shown in **Figure 1** [8,9], it dissolves easily in water and has solubility as well in methanol and ethanol [10].

Captopril is a preferred treatment for many doctors due to its therapeutic benefits, efficacy, and low commercial price [11]. It's mainly used for the treatment of arterial hypertension, heart failure [12-14], diabetic nephropathy [15], and some other diseases resulting from heart failure [16]; it's widely used by geriatric patients who suffer from these diseases [17].

Captopril may cause side effects such as coughing [18]. Captopril has been quantified by more than one analytical method, including spectrophotometry [19-22], flow injection methods [23-28], RP-HPLC [29,30], and HPLC [31-33].

Some of these methods are not simple for routine analysis, requiring expensive or complex tools. Analytical systems by flow injection are more suitable for everyday use in quality control laboratories for the production of pharmaceutical preparations due to their simplicity of work, speed, sensitivity, and less consumption of reagents, sample samples, and other chemicals when compared to other methods of chemical analysis. This study describes a simple, sensitive, fast, low-contamination, easy-to-operate analytical method for determining CAP within the continuous flow injection analysis (CFIA) technique [34-40].

Captopril was estimated after its interaction with ammonium by studying the precipitate formed as a result of the oxidation of CAP in an acidic medium using homemade Ayah 6SX1-ST-2D solar cell CFI analyzer [41], which was used in previous studies for the determination of some drugs [42-47].

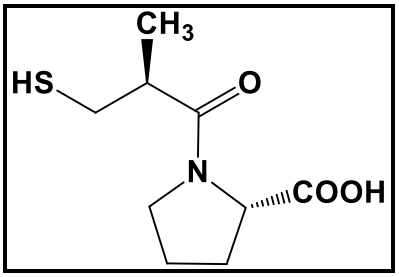

Figure 1. Molecular structure of captopril

2. Materials and Methods

2.1 Reagents and chemicals

In this study, all chemicals of the analytical class were used, and the preparation was done using distilled water as a solvent. A stock solution of Captopril ($C_9H_{15}NO_3S$, M.Wt 217.29 g/mol, SDI, 10 mmol/L) the preparation was done by dissolving 0.21729 g in 100 mL distilled water. A stock solution (20 mmol/L) of ammonium ceric sulfate $2(NH_4)_2SO_4$ $Ce(SO_4)2.31/2$ H_2O (M.Wt 659.62 g/mol, Hopkin & Williams) preparation was done by dissolving 6.5962 g in 500 mL of distilled water. A 100 mmol/L from each of the following acids (supplied from BDH) sulfuric acid solution

(98% w/w, 1.84 g/mL), hydrochloric acid solution (35% w/w, 1.19 g/ml), nitric acid solution (70% w/w, 1.42 g/mL), acetic acid solution (99.5% w/w, 1.05 g/mL). (100mmol/L) from each of the following salts (supplied from BDH): NaCl (M.Wt 58.44 g/mol, BDH), $NaNO_2$(M.Wt 68.9953 g/mol, BDH), $NaNO_3$ (M.Wt 84.9947 g/mol, BDH), NH_4Cl (M.Wt 53.491 g/mol, BDH), Na_2CO_3 (M.Wt 105.99 g/mol, BDH).

2.2 Sample preparation

Twenty tablets of each pharmaceutical preparation were crushed using a ceramic mortar and sieved through a 200-mesh sieve. Each of the drugs containing (25 mg) CAP (provided by SDI-Iraq, Pioneer Pharmaceutical-Iraq, and Medochemi-Cyprus) weighed (1.2186, 0.9447, and 1.1612) g, respectively. According to the proportional relationship for each preparation, each of the weights above is equivalent to (0.21729 g) of the active substance to obtain a solution with a concentration of (10 mmol/L) of each pharmaceutical preparation. With continuous stirring, the powder was dissolved in distilled water. After the dissolution, the volume was completed to (100 mL) with distilled water. Then, the prepared solution was filtered to eliminate any undissolved material that may affect the result.

2.3 Apparatus

The apparatus used in the new method for CAP determination consists of a two-channel variable speed peristaltic pump (Supplied from Ismatec, Switzerland) and a six-hole medium-pressure injection valve (Supplied from IDEX corporation, U.S.A.) with a sample loop (0.7 mm i.d. Teflon, different length). Ayah 6S×1-T-2D Solar cell CFI analyzer (Homemade) The response was measured by it; three pairs (6) snow white LEDs are used as the beam source in the flow cell where the path length 2 mm, as a detector to collect signals via a 60 mm travel-sample, two solar cells were used. The response is output in the form of peaks through the x-t potentiometric recorder (Kompenso Graph C-1032, supplied from Siemens-Germany) (1-500 volt, 1-500 mV), the flow diagram for the determination of CAP is shown in **Figure 2**. For measurements, the UV-Spectrophotometric method used a UV-Vis spectrophotometer (Shimadzu double beam. In this device, the wavelength scanning range was 190-1100 nm, and the 1 mL measuring cell was made of quartz, model UV-180^0 Kyoto-Japan).

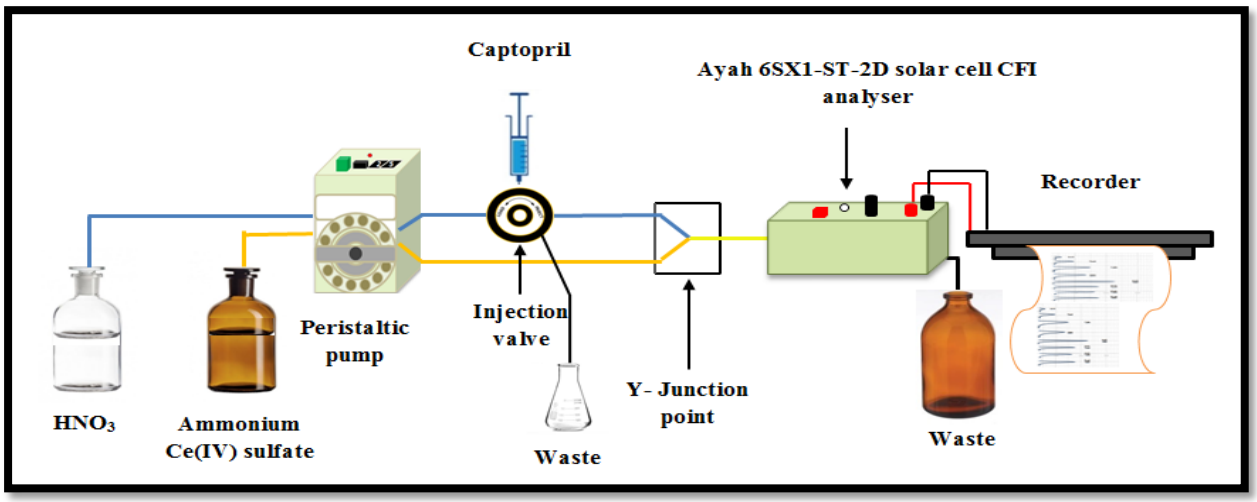

Figure 2. Flow diagram for the system used to determine captopril

Two lines make up the manifold flow system in **Figure 2** for determining CAP by direct oxidation in an acidic medium with ACS, where a slightly yellowish precipitate was formed. The first line provided nitric acid (200 mmol/L), which is a carrier stream at (1.5 mL/min) connected to the injection valve for hold CAP (used sample volume 25 µL), the second line carried ACS

(10 mmol/L) at 1.5 mL/min. The second line meets the first line (which the CAP solution is injected into) at the Y-Junction, and reaction products outlet from it to pass through the Ayah 6S×1-ST-2D Solar cell CFI analyzer. Each solution was injected three times in succession. An x-t potentiometric recorder was used to capture the response diagram, where the responses appeared in the form of peaks expressing the transducer's response and the peak height representing the amount of light reflected after it fell on the surface of the sediment particles in the flow cell. A proposed CAP oxidation mechanism by ACS in an acidic reaction medium is present in **Sketch 1** [16,17,48].

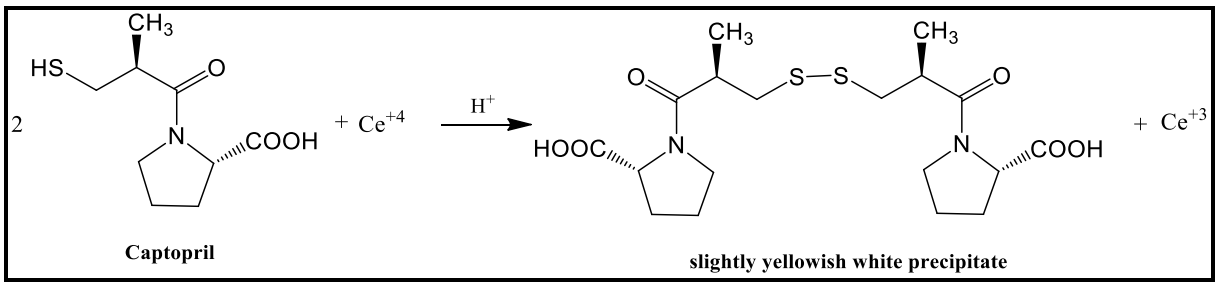

Sketch 1. The suggested mechanism of the CAP and ACS reaction in acidic medium

3. Results and Discussion

The concentration of the ACS reagent, the selection of the type of reaction medium (carrier stream), and the concentration of the optimal medium (nitric acid) were mainly studied to determine some of the optimal chemical parameters. Meanwhile, the flow rate and sample volume were studied to resolve some optimal physical parameters. By making it constant and variable each time these variables were optimized.

3.1 Chemical variables

3.1.1 Effect of ACS concentration

A series of concentrations of ACS (1-20) mmol/L was prepared. A 2 mmol/L of CAP was injected using a sample volume of 25µl and distilled water as carrier stream; 2.3 ml/min was the flow rate for each of the reagent lines and carrier streamline. All measurement was refined three times. The response outline for this experience is shown in **Figure 3A**, and **Figure 3B** shows the effect of ACS concentration on the peak rise average of the response's transducer. The results were compacted in **Table 1**. The results found that the highest response appeared at the concentration of (10 mmol/L), so it was determined as an optimal concentration of the reagent. **Figure 3** shows the outline of the result using Ayah 6S×1-ST-2D Solar cell-CFI analyzer; the responses of white precipitate increase ascendingly with a rise in concentration of ACS until reaching a concentration of 10 mmol/L, then the reaction begins to gradually decrease after this concentration (> 10 mmol/L) of ACS; this may be attributed to increasing in the amount of sediment, which causes slow movement of its particles and an increase in the aggregation of those particles, mainly causing accumulation of precipitate particles in front of the detector which in turn to a decrease in reflecting surface, this results in a reduction of peak height.

From **Figure 3A**, it is clear that the peak of response was higher and the width of the baseless, so the concentration of 10 mmol/L was chosen for the subsequent experiments as the optimal concentration of the reagent (ACS). **Figure 3B** shows ACS concentrations on the transducer response peak rise rate in (mV).

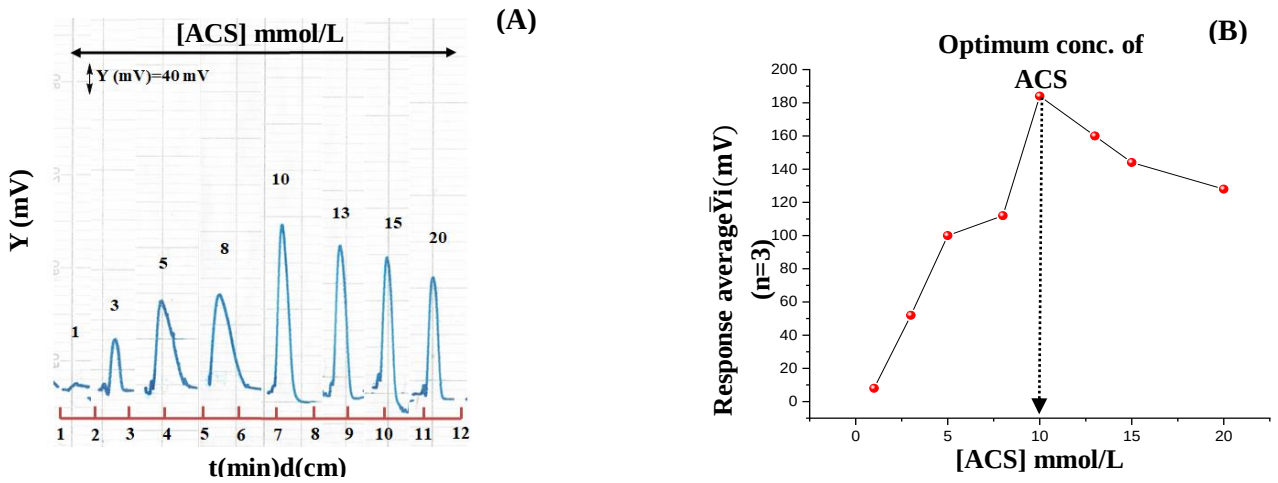

Figure 3. ACS concentration's effect on : **A:** response outline versus time. **B:** Peak rise rate of transducer response in (mV)

Table1. Synopsis of the results of effect of the concentration of ACS reagent on the responses average of the transducer

[ACS] mmol/L	Response average $\bar{Y}i$(mV)for (n=3)	R S D %	Interval of confidence at (95%),n-1 $\bar{Y}i \pm t_{0.05/2,n-1}\frac{\sigma_{n-1}}{\sqrt{n}}$
1	8	0.2051	8 ∓ 0.0407
3	52	0.2001	52 ∓ 0.2586
5	100	0.2212	100 ∓ 0.5495
8	112	0.2301	112 ∓ 0.6402
10	184	0.2312	184 ∓ 1.0568
13	160	0.2340	160 ∓ 0.9301
15	144	0.2190	144 ∓ 0.7834
20	128	0.2132	128 ∓ 0.6779

$\bar{Y}i_{(mV)}$(S/N) response of an energy transducer in (mV) for n=3,$t_{tab0.05/2,2}$=4.303.R.S.D%:relative standard deviation, σ_{n-1}:standard deviation, n: the number of repetitions of the measurement, Interval of confidence: A range of values above and below the point estimate within which the true value in the population is likely to lie with 95%.

3.1.2 Effect of different medium

To determine the optimal reaction medium between CAP (2 mmol/L) with ACS (10 mmol/L), different solutions were used as carrier current (CH_3COOH, HCl, HNO_3, H_2SO_4, NaCl, NH_4Cl, $NaNO_2$, $NaNO_3$, Na_2CO_3). At a concentration of 0.1 mol/L and in the aqueous medium. It was observed in the study that the response plot over time in this experiment showed variation in the intensity of the S/N response (variation in the height of the peaks). The plot also showed that the highest response was when nitric acid was used as the reaction medium (carrier current). This may be due to the small and uniform size of the deposited particles, in other words, the increased reflective surface area. Therefore, the medium HNO_3 solution was used as the carrier current in the following experiments. The responses that demonstrated this are shown in **Figure 5A**.

Figure 5B Schematic showing the effect of medium change on the average response of the transducer. **Table 2** summarizes the results of the impact of the type of medium.

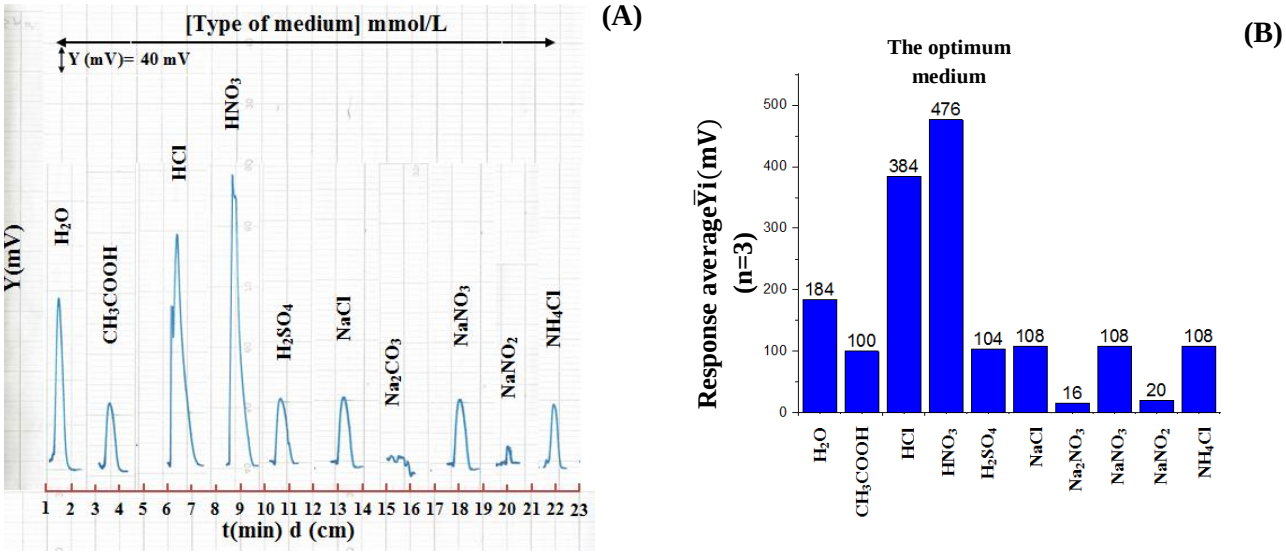

Figure 4A. Response outline versus time explain the effect of different media. **B:**A graphical diagram showing the effect of medium change on the response average of a transducer

Table 2. A synopsis of the effects of several medium types on the transducer's average responses

[Medium type] mmol/L	Response average $\bar{Y}i$(mV)for (n=3)	R S D %	Interval of confidence at (95%),n-1 $\bar{Y}i \pm t_{0.05/2,n-1}\frac{\sigma_{n-1}}{\sqrt{n}}$
H_2O	184	0.2312	184 ∓ 1.0568
CH_3COOH	100	0.2100	100 ∓ 0.5217
HCl	384	0.2200	384 ∓ 2.0987
HNO_3	476	0.2016	476 ∓ 2.3849
H_2SO_4	104	0.2001	104 ∓ 0.51699
NaCl	108	0.2200	108 ∓ 0.5903
Na_2CO_3	16	0.2100	16 ∓ 0.0835
$NaNO_3$	108	0.2100	108 ∓ 0.5680
$NaNO_2$	20	0.2000	20 ∓ 0.0994
NH_4Cl	108	0.2201	108 ∓ 0.5905

3.1.3 Effect of HNO_3 concentration

Using CAP (2 mmol/L)-ACS(10 mmol/L) system within the range (20-240 mmol/L) a series of solutions of nitric acid were prepared; the sample volume was (25 µL) at a flow rate (of 1.5 mL/min) for both of the first lines (carrier stream) with the second line (reagent). **Figure 4A** shows the effect of HNO_3 concentration on the responses in the response outline, and **Figure 4B** shows the effect of HNO_3 concentration change on the peak rise rate of the transducer response. Experiment results are compacted in **Table 2**. It was observed through the increased intensity of the reactions shown in **Figure 5A**. (20 mmol/L) from HNO_3 it was the first solution to be measured, and what is observed in Figure 5B is that the response increases by increasing the concentration until reaching concentration (200 mmol/L), which indicates that the acid was necessary because of its effect stimulating the reaction, the complete dissolution of the ACS salt and to ensure complete homogeneity. The concentration (200 mmol/L) gave the peak's highest response and the lowest width. Therefore, the concentration (200 mmol/L) of HNO_3 was selected as the optimal concentration for the optimum carrier stream in the subsequent experiments.

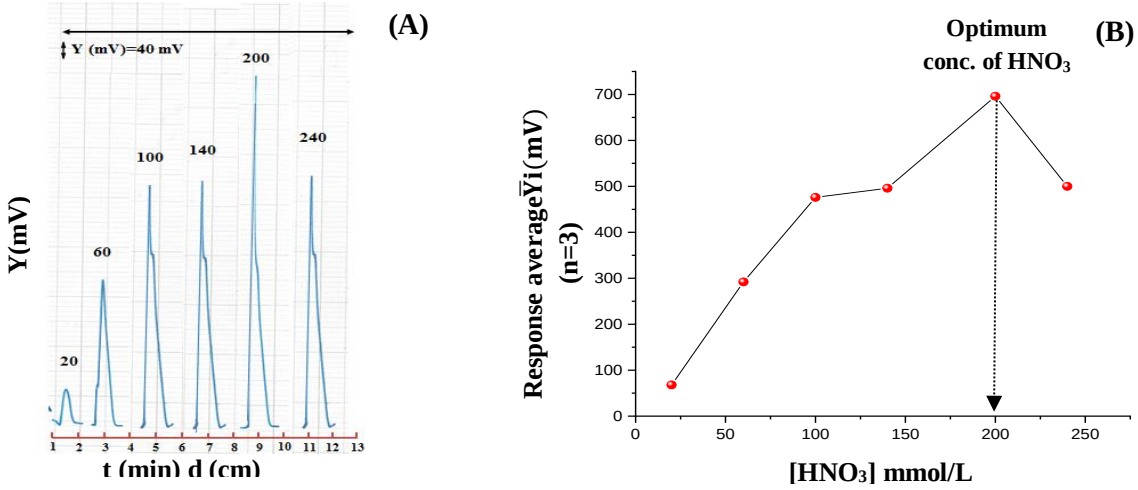

Figure 5. HNO3 concentration's effect on: **A**: response shape against time . **B**: Peak rise rate of transducer response in (mV)

Table 3. Synopsis of the results of responses to effect of HNO_3 concentration on the responses average of the transducer

[HNO_3] mmol/L	Response average $\bar{Y}i$(mV)for (n=3)	R S D %	Interval of confidence at (95%),n-1 $\bar{Y}i \mp t_{0.05/2}\sigma_{n-1}/\sqrt{n}$
20	68	0.2941	68 ∓0.4968
60	292	0.2911	292 ∓ 2.1116
100	476	0.2016	476 ∓ 2.3849
140	496	0.1411	496 ∓ 1.7390
200	696	0.1408	696 ∓ 2.4346
240	500	0.1760	500 ∓ 2.1862

3.2 Physical variables

3.2.1 Flow rate

The optimal flow rate was studied within the range (1.0- 2.5) mL/min for both line (carrier streamline) and line 2 (reagent line); a peristaltic pump was used to control the flow rate for determination of CAP at (2 mmol/L). The study was carried out by fixing the other parameters (i.e., 10 mmol/L from ACS, 0.2 mmol/L from HNO_3 as the best carrier stream, sample volume was 25 µL, and open valve (10 sec). The results of the experiment were compacted in **Table 4**. A slow flow rate (1 mL/min) was shown to generate an increase in dilution and dispersion, which may have led to the rise in the base width of the response ΔtB, While the flow rates higher than (1.5 mL/min) showed a gradual decrease in the response with irregularity in the peaks of some responses, this may be attributed to the fact that at high speed the sample retention time with the detector is reduced. It is the least possible. This leads to a decrease in the amount of light reflected towards the sensor, which reduces the intensity of the response. **Figure 6A** shows a plot of the transducer response against time. **Figure 6B** shows the effect of changing flow rate on the rate of peak rise of the transducer response, base width, and arrival time to the measuring flow cell. It was found from the two charts that the highest response was recorded at the pump speed 10 (1.5 mL/min), so it was chosen as the optimal speed in the subsequent experiments.

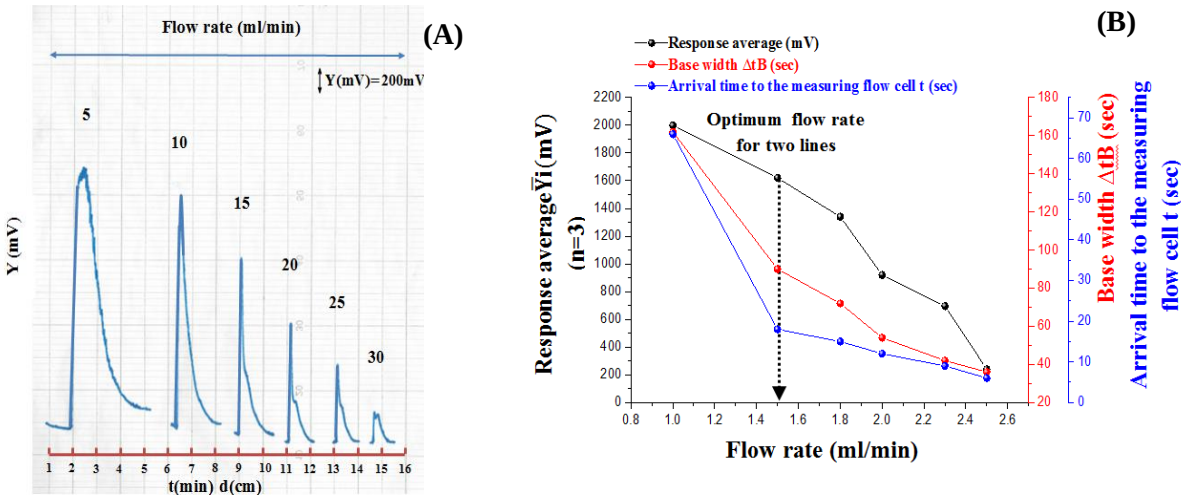

Figure 6. Flow rate's effect on: **A:** response outline against time . **B:** Peak rise rate of transducer response in (mV) and base width

Table 4. An synopsis of the findings showing how changing flow rate affected the transducers' average responses

pump speed	Flow rate (ml/min) both two lines	Response average $\bar{Y}i$(mV) (n=3)	R S D%	Interval of confidence at 95% $\bar{Y}i \pm t_{0.05/2}.\frac{\sigma_{n-1}}{\sqrt{n}}$	t (sec)	Base width ΔtB (sec)	V_{add} (ml) In flow cell	Conc. (mmol/L) In flow cell	D_f
5	1.0	2000	0.1050	2000∓ 5.2171	66	162	5.4250	0.0092	217.3913
10	1.5	1620	0.1111	1620 ∓ 4.4718	18	90	4.5250	0.0110	181.8181
15	1.8	1340	0.1044	1340 ∓ 3.4780	15	72	4.3450	0.0115	173.9130
20	2.0	920	0.1195	920 ∓ 2.7327	12	54	3.6250	0.0138	144.9257
25	2.3	696	0.1408	696 ∓ 2.4346	9	42	3.2450	0.0154	129.8701
30	2.5	240	0.1041	240 ∓ 0.6210	6	36	3.0250	0.0165	121.2121

t: Time arrival estimated from the injection valve to the measurement cell (sec),Δt: Base width of peak(sec), V_{add}: Addition volume(ml)in flow cell, D_f: Dilution factor in flow cell.

3.2.2 Sample volume

With the use of optimum flow rate (1.5 mL/min) for both the carrier stream with ACS reagent line, CAP (2 mmol/L)-ACS (10 mmol/L)-HNO_3 (200 mmol/L) system. Various volumes of injected sample were used within the range (20-100) µL, open valve 10 sec. It was observed through the transducer's responses outline against time there was an apparent increase in the intensity of the reaction at sample volume 25 µL, as shown **in Figure 7A, B** where the highest peak appeared. A synopsis of the results of the experiment is shown in Table 5. Increasing the sample volume (to more than 25 µL) might lengthen the sample piece's exposure to the detector. This would likely result in an irregular flow of two factors, dispersion, and convection, allowing the convective current to continue and causing the precipitating particles to migrate backward. If the reflective surface weren't damaged somehow, it would still be able to reflect the light from the incident source. According to this potential explanation, the response peak height would be smaller, and the peak profile would be broad. **Figure 7A** shows a plot of the transducer response against time. At the same time, **Figure 7B** shows the effect of changing sample volume on the rate of peak rise of the transducer response, base width, and arrival time to the measuring flow cell. It was found from the two charts that the highest response was recorded at the sample volume of 25 µL, so it was chosen as the optimal sample volume in the subsequent experiments.

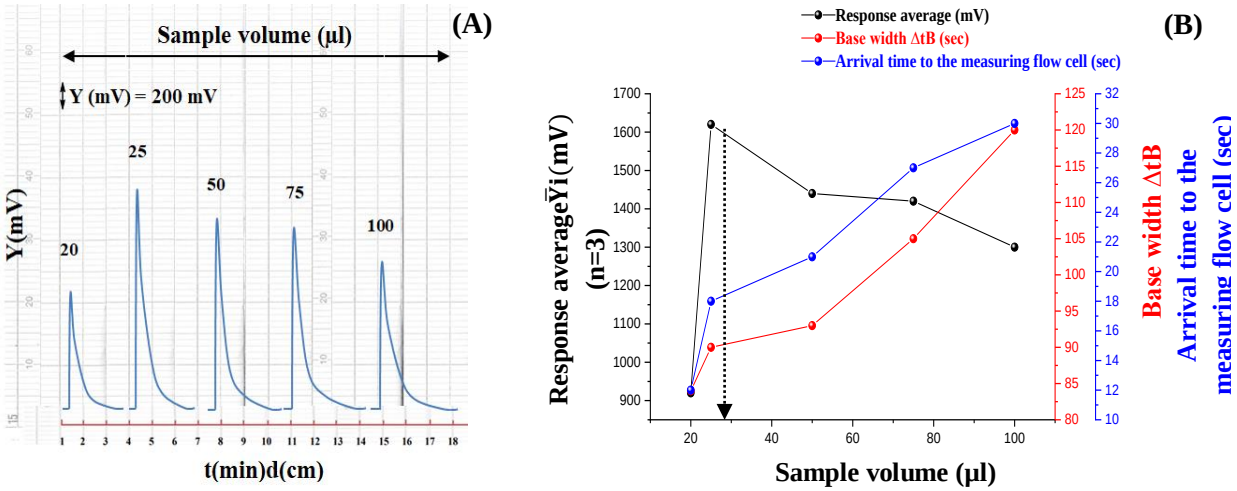

Figure 7. Sample volume's effect on: **A:**Outline's response against time . **B:** Peak rise rate of transducer response in (mV) and base breadth

Table 5. Synopsis of the results of the effect of the difference in the sample volume on the average of transducer's responses

Sample volume (µl)	Response average $\bar{Y}i$(mV) (n=3)	R S D %	Interval of confidence at (95%), n-1 $\bar{Y}i \pm t_{0.05/2}.\frac{\sigma_{n-1}}{\sqrt{n}}$	t (Sec)	Base width ΔtB (Sec)	V_{add} (ml) In flow cell	Conc. (mmol/L) In flow cell	D_f
20	920	0.1108	920 ∓ 2.5340	12	84	4.4000	0.0090	222.222
25	1620	0.1111	1620 ∓ 4.4718	18	90	4.5250	0.0110	181.8181
50	1440	0.1138	1440 ∓ 4.0743	21	93	4.7000	0.0212	94.3369
75	1420	0.1140	1420 ∓ 4.0246	27	105	5.3250	0.0281	71.1743
100	1300	0.1230	1300 ∓ 3.9749	30	120	6.1000	0.0327	61.1620

t: Time arrival estimated from the injection valve to the measurement cell (sec), Δt: Base breadth of peak(sec), V_{add}: Addition volume(ml)in flow cell, D_f: Dilution factor in flow cell.

3.3 Calibration curve (scatter plot) for variance of CAP concentration against transducer response

The optimal chemical and physical parameters were adopted to prepare a series of CAP solutions within the range (0.07-10) mmol/L, the measurement was repeated for each concentration three successive times. Responses are shown as in **Figure 8A** which shows the response range and peak height for each concentration of CAP. As shown in **Figure 8B** the linear calibration was within the range (0.07-3) mmol/L, accompanied by a correlation coefficient (r)= 0.9983. The obtained results show the linear regression of the change of transducer response against the change of CAP concentration as in **Table 6**, the equation that was used in this part of the study was $\hat{y} = a + bx$ [49] (First degree equation). The value of t was calculated at a confidence level (95%) , which was greater than the value of the tabular t, which leads us to say that linearity versus nonlinearity is acceptable.

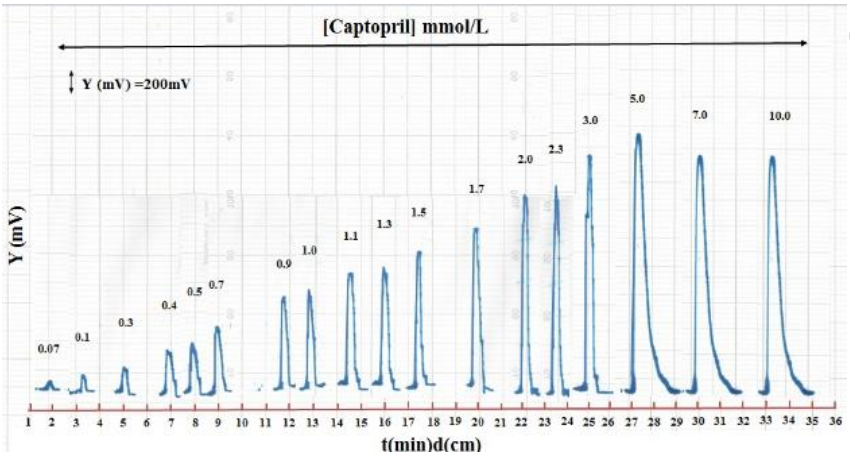

(A)

Figure 8A. A calibration curve shows the effect of CAP concentration change against time on transducer response (for some responses)

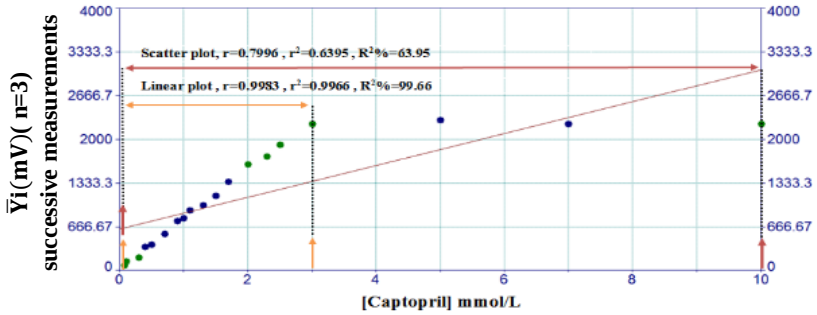

(B)

Figure 8B. Scatter and linear plot of the new method expresses the transducer response against conc. by linear equation

Table 6. Synopsis of results the transducer response average against changing CAP concentration using first degree equation

Type of mode	Range of [CAP] mmol/L	$\hat{Y}$(mV) =a ±Sa.t+b±Sb.t[CAP]mmol/L at 95%.n-2	r r^2 R^2%	t_{tab} at 95%, n-2	$t_{cal}=\frac{\lvert r\rvert\sqrt{n-2}}{\sqrt{1-r^2}}$
Scatter plot	0.07-10 (n=19)	629.1921±310.3027 + 243.3006 ± 93.4715[CAP]	0.7996 0.6395 63.95	2.110<5.4910	
Linear range	0.07-3 (n=16)	45.8635±37.3236+748.8995±25.0941[CAP]	0.9983 0.9966 99.66	2.145<<63.1962	

n:number of measurement ,$\hat{Y}$(mV):estimated value of cell in(mV) , r:Correlation coefficient, r^2:Coefficient of determination, R^2%:Explained variation as a percentage / total variation, $t_{tab}=t_{0.05/2,n-2}$

3.4 Limit of detection (L.O.D)

The method's detection limit is the minimum concentration that the device can sense. A study determined the CAP detection limit through three methods: practically based on diluting to the minimum concentration gradually, theoretically based on the slope value, use, and on the base of the linear equation, as shown in **Table 7** at optimum parameters.

Table 7. Method's detection limit value for CAP

Practically based on the progressive dilution for the minimal concentration (0.07)mmol/L	Theoretical in accordance with the slope value X=3S_B/Slope , n=16	Based of linear equation $\hat{Y}=Y_b + 3S_b$
272.5 ng /25µL	6.5277 ng /25µL	877.5 ng /25µL

X= limit of detection value , SB=standard deviation value of blank refined for 16 times, Y_b: average response for blank=intercept(a), S_b: Standard deviation equal to Sy/x(residual) from linear range ,$\hat{Y}$:estimated response (mV).

3.5 Repeatability

Equivalent percentage equivalent to the test-retest measurement reliability expresses the relative standard deviation. The responses were re-measured for each concentration through eight consecutive injections for three stable CAP concentrations (0.9, 1.5, and 3.0) mmol/L in optimum conditions for n=8. The response profile is shown in **Figure 9**. **Table 8** displays that the relative standard deviation as a percentage was less than 0.2%, making it abundantly evident that the suggested approach and instrument were suitable for determining CAP.

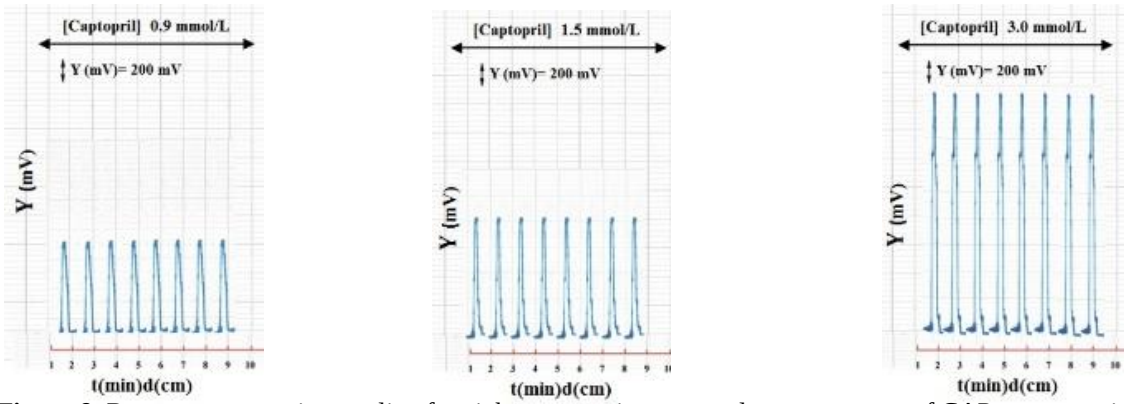

Figure 9. Response versus time outline for eight consecutive repeated measurements of CAP concentration (0.9,1.5,3.0) mmol/L

Table 8. Synopsis of results for repeatability of CAP at optimal parameters

[CAP] mmol/L	Response average $\bar{Y}$i(mV)for (n=8)	R S D %	Interval of confidence at 95% $\bar{Y}i \pm t_{0.05/2,n-1}.\frac{\sigma_{n-1}}{\sqrt{n}}$
0.9	760	0.1052	760± 0.6689
1.5	1140	0.1052	1140 ± 1.0033
3.0	2240	0.1026	2240 ±1.9231

$t_{tab0.05/2,7}$=2.365, n: the number of repetitions of the measurement

3.6 UV-Spectrophotometric method (Classical method)

To evaluate the new method (CFIA), a comparison was made between it and one of the analytical methods, specifically the UV spectrophotometry method based on absorption value measurements. The concentration extent of the method was (0.002-0.150) mmol/L at λmax= 207.2 nm (at 0.028 mmol/L) **Figure 10** using quartz cell. **Figure 11** shows the scatter plot was from (0.002-0.150) mmol/L while the linear range was (0.002-0.09) mmol/L. Correlation coefficient (r)= 0.9995 and R^2%=99.90, n=18 (n= number of measurements). L.O.D. was 217.29 ng/1000 µL, calculated by gradual dilution to the lowest concentration in the calibration curve (0.002 mmol/L). The summary of the method results is in **Table 9**.

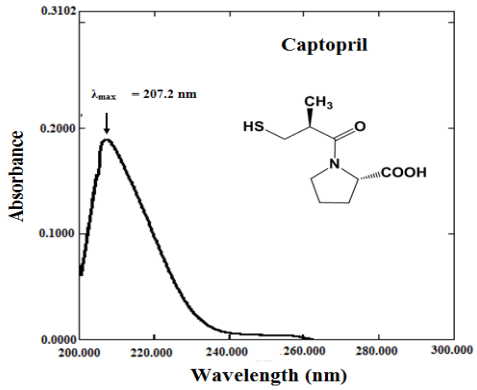

Figure 10. Absorbance of UV-Spectrum of CAP at concentration 0.028 mmol/L that shows λmax=207.2 nm

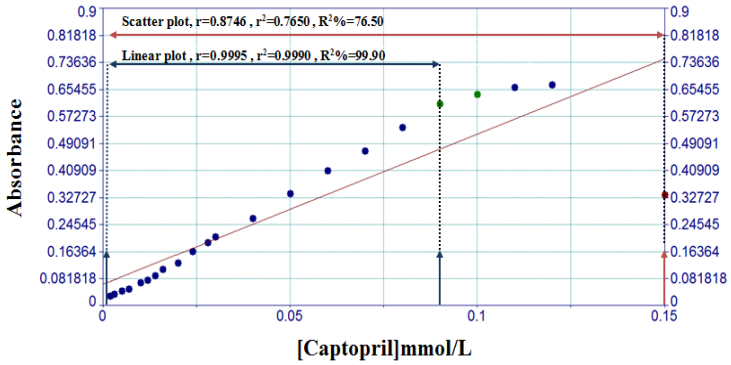

11. Scatter plot at (0.002-0.15) mmol/L, n=22 for CAP using classical method at 207.2 nm, in addition to linear range at (0.002-0.09)mmol/L for n=18

Table 9. Synopsis of linear regression for the determination of CAP using UV-Spectrophotometric method (classical method)

Type of mode	Extent in calibration curve	n	linear regressive at Interval of confidence 95%,n-2 $\hat{Y}$=a±Sa.t+b($\Delta y/\Delta x_{mmol/L}$)±bt [CAP]mmol/L	r r^2 R^2%	t_{tab} at 95% ,n-2	$t_{cal}=\frac{\lvert r\rvert\sqrt{n-2}}{\sqrt{1-r^2}}$	L.O.D.
Scatter plot	0.002-0.150	22	0.0639±0.0750+4.5582±1.1779[CAP]	0.8746 0.7650 76.50	2.086<8.0695		
Linear plot	0.002-0.09	18	0.0052±0.0048 +6.6818±0.1185[CAP]	0.9995 0.9990 99.90	2.120 << 126.5189		217.29 ng/1000µ

n:number of measurement ,$\hat{Y}$(mV):estimated value without unite on spectrophotometric , r:Correlation coefficient, r^2:Coefficient of determination, R^2%:Explained variation as a percentage / total variation, $t_{tab}=t_{0.05/2,n-2}$, L.O.D.: Limit of detection.

3.7 The CAP-ACS-HNO_3 system evaluation for the CFIA method (new method) for determining captopril in pharmaceutical preparations

To evaluate the efficiency of the new method, which was made using Ayah 6S×1-ST-2D Solar cell CFI analyzer (homemade), to determine CAP in pharmaceutical preparations. Five solutions were prepared for each drug for samples from three different companies for the production of pharmaceutical preparations (SDI-Iraq, Pioneer-Iraq, and Medochemi-Cyprus), where comparison was made with the UV-Spectrophotometric method(classical method) after applying the method of standard additions to both the two methods are as follows:

For the new method: five volumetric flasks of (10 mL) were prepared and (1.0 mL from 10 mmol/L) was transferred into each of them, after which different volumes of the captopril's standard solution were gradually added (S.D.I.-Iraq) (0.0, 0.5, 1.0, 1.5, 2.0) mL of (10 mmol/L) to gain (0.0, 0.5, 1.0, 1.5, 2.0) mmol/L.

For the classical method: five volumetric flask of (10 mL) were prepared and (0.5 mL from 1.0 mmol/L) was transferred into each of them, after which different volumes of captopril's standard solution were gradually added (S.D.I.-Iraq) (0.0, 0.1, 0.2, 0.3, 0.4) mL of (1.0 mmol/L) to gain (0.0, 0.01, 0.02, 0.03, 0.04) mmol/L. Flask number 1 is a sample. Measurements were made for both methods. The results obtained from the standard addition method were treated statistically. The results are summarized in **Table 10A** and **B** at a confidence level (95%). To determine whether

there is a significant difference, the t-test and the F-test were performed, and the results were processed statistically [49]. The results of the t-test and F-test were summarized in **Table 10B** (columns 4 and 5). Results showed there was no significant difference between the new method and the classical method at 95% of the level of confidence. A t-calculated (-1.373) is less than the t-tabular (4.303), as well as the calculated F-value (8.7064) is less than the tabular F-value (39) [50]. **Figure 12** is a graphical chart showing how changing the CAP concentration (using the standard addition method) affects the S/N transducer's response against time.

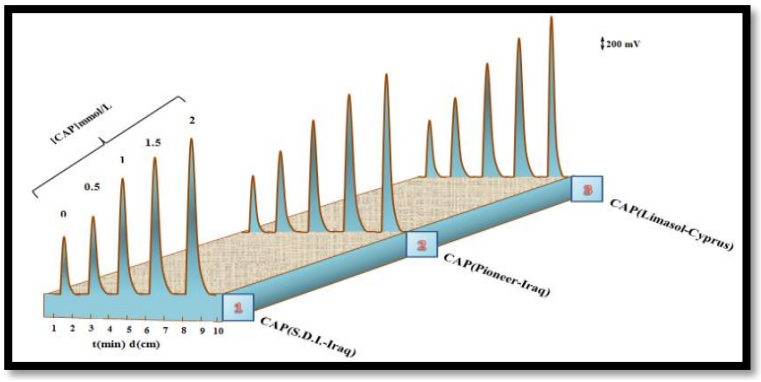

Figure 12. Effect of variation of captopril concentration (using standard addition method) on S/N energy transducer response versus time(min),distains (cm) for three sample drugs using Ayah 6S×1-ST-2D solar cell CFI analyser . 1-Iraq, Captosam, S.D.I., 2-Iraq, Captoneer, Pioneer, 3-Cyprus, Rilcaptoo. Limassol

Table 10A. Synopsis of results standard addition in three pharmaceutical preparations for new method and classical method.

No. of sample	Commercial name Company Content Country	Type of method: New method — UV-Sp. Method absorbance measurements at λ_{max}= 207.2 nm										
		Confidence interval for the Weight of Tablet $\bar{w}i \pm 1.96\sigma n\text{-}1/\sqrt{n}$ at 95% (g)	Weight of the sample is equivalent to 0.21729 (g) (10 mmol /L) of the active ingredient Wi (g)	Theoretical content for the active ingredient at 95% (mg) $Wi \pm 1.96\sigma n\text{-}1/\sqrt{n}$	Captopril					Standard addition equation at 95% for n-2	r r^2 R^2%
					0 mL	0.5 mL	1.0 mL	1.5 mL	2.0 mL	$\hat{Y}$ (mV) $=a_{mV} \pm Sa.t + b(\Delta y_{mV}/\Delta x mmol/)b.t$ [Captopril]mmol/L	
					0 mmol /L	0.5 mmol /L	1.0 mmol /L	1.5 mmol /L	2.0 mmol /L		
					0 mL	0.1 mL	0.2 mL	0.3 mL	0.4 mL	$\hat{Y} = a \pm Sa.t + b(\Delta y / \Delta x$ mmol/L $) \pm Sb.t$ [Captopril] mmol/L	
					0 mmol /L	0.01 mmol /L	0.02 mmol /L	0.03 mmol /L	0.04 mmol /L		
1	Captosam S.D.I 25 mg Iraq	0.14021±0.0010	1.2186	25±0.1930	790 mV 0.342	1100 mV 0.412	1590 mV 0.478	1910 mV 0.540	2230 mV 0.613	752 ±66.5941+758±54.3740[CAP]mmol/L 0.343 ±0.0070+6.700±0.2959 [CAP]mmol/L	0.9992 0.9984 99.84 0.9996 0.9994 99.94
2	Captoneer Pioneer 25 mg Iraq	0.1087±0.0007	0.9447	25±0.1769	750 mV 0.324	1050 mV 0.401	1550 mV 0.450	1900 mV 0.520	2220 mV 0.602	736±137.3058+758±112.1098 [CAP]mmol/L 0.3244±0.0235+6.7500±0.9660[CAP]mmol/L	0.9967 0.9935 99.35 0.9969 0.9939 99.39
3	Rilcaptoo Limassol 25 mg Cyprus(EU)	0.1336±0.0003	1.1612	25±0.06831	780 mV 0.360	1110 mV 0.440	1585 mV 0.501	1915 mV 0.570	2235 mV 0.645	760±70.6874+761±57.7160 [CAP]mmol/L 0.3632±0.0120+7.0000±0.5024 CAP]mmol/L	0.9991 0.9982 99.82 0.9991 0.9984 99.84

$\hat{Y}$: Estimated response in (mV) for the new method and the UV-Sp.method absorbance value, r: correlation coefficient, R^2%: variance explained in percentage /total variation, UV-Sp. :UV-Spectrophotometric method, $\bar{w}i$: Practical weight in(mg), $t_{tab}= t_{0.05/2,\infty}$ =1.960 at 95%,$t_{tab}= t_{0.05/2,3}$= 3.182 for n=5,using volume of cell (quartz) 1 mL in UV-Spectrophotometric method.

Table 10B. Synopsis of practical content results ,percentage recovery (Rec.%) for CAP determination in three pharmaceutical preparations, t-test and F-test

No. of sample	Type of method: New method — UV-Sp. Classical method Absorbance measurement at 207.2 nm: Workable concentration (mmol/L) In 10 mL / In 100 mL	Type of method: New method — UV-Sp. Classical method Absorbance measurement at 207.2 nm: Efficiency of determination Rec.%	t-test: $t_{cal}=\frac{\bar{X}d}{\sigma_{n-1}}\sqrt{n}$	t-test: t_{tab} at level of confidence 95%	F-test: $F_{cal}=S^2_2/S^2_1$	F-test: F_{tab}
	0.9920 / 9.9200	99.1728				
1	0.0514 / 10.286	102.84	$\bar{X}d$= - 0.5510 σ_{n-1}=0.6953 |-1.373| < 4.303		σ^{**}_{n-1}=0.3546 , S_1^2(CFIA) =0.1257 σ^{*}_{n-1}=1.0461 , S_2^2(UV-Sp.)=1.0944 8.7064 < 39.0000	
	0.9709 / 9.7097	97.1039				
2	0.0480 / 9.6100	96.1006				
	0.9986 / 9.9860	99.8200				
3	0.0518 / 10.377	103.7688				

$\bar{X}d$: Comparing two types of methods, on average (new & classical) ,n(no. of sample)=3,σ_{n-1}:standard deviation of different (paired t-test), $t_{tab}=t_{0.05/2,2}$=4.303 (for paired t-test), $F_{tab}= F_{0.95,V1,V2}= F_{0.95,2,2}$=39, σ^{**}_{n-1} : standard deviation for new method, σ^{*}_{n-1} standard deviation for classical method (F-test),$S^2_{1(CFIA)}$:Variation of new method, $S^2_{2(UV\text{-}Sp.)}$:Variation of classical method. UV–Sp.: UV–Spectrophotometric method .

4. Conclusion

The method presented in this work is simple, sensitive, fast and meets part of the requirements of green chemistry. It has been successfully applied for the determination of CAP in pure and pharmaceutical preparations based on the reaction of CAP with ACS in acidic media. An alternative analytical method for estimating CAP was reached through this study, which was conducted under simple conditions and parameters using Ayah 6SX1-ST-2D solar cell CFI analyzer .

Acknowledgment

After the completion of the study, the authors extend their thanks and appreciation to (S.D.I.) for providing the pure sample of the drug for free to the Department of Chemistry in the College of Science/ University of Baghdad to facilitate the task of completing some of the research requirements and to Prof.Dr. Issam M. Ali Al-Hashemi for his distinguished scientific effort in designing the Ayah 6SX1-ST-2D solar cell CFI analyzer, by which the work methodology in this study was completed.

Conflict of Interest

The authors declare that they have no conflicts of interest.

Funding: None

References

1. Proth, C.M. Pathophysiology, Concepts of altered health States.7th ed. St. Lippincott Williams and Wilkins:Philadelphia,**2005**. https://library.villanova.edu/Casa/Record/1695408/Details?sid=2019237.
2. Christian, O.; Roland E. S. Diagnosis and treatment of arterial hypertension **2021**. *Kidney international*.**2022**;*101(1):* 36-46. https://doi:10.1016/j.kint.2021.09.026.
3. Bushra, B.Q. ; Ahmed, A.A. Indirect way for the assay of captopril drug in dosage forms using1,10-phenanthroline as a selective spectrophotometric agent for Fe(II) via homemade CFIA/merging zones technique. *Ibn Al-Haitham Journal for Pure and Applied science*, **2017**, 294-320. https://www.iasj.net/iasj/download/fb43ee37619ebfee.
4. Weronika, F.; Armanda, W.; Wiktoria, L.; Ewelina, M.; Beata, F.; Jacek, R. Pathophysiology of Cardiovascular Diseases: New Insights into Molecular Mechanisms of Atherosclerosis, Arterial Hypertension, and Coronary Artery Disease. *Biomedicines*. **2022;***10(8)*,1-17. https://doi:10.3390/biomedicines10081938.
5. Denilson, M.O.;Willian, T.S. ,Benedito, R.; Wesley, L.G. ;Vagner, B.S. Nitroprusside as a novel reagent for flow injection spectrophotometric determination of captopril. *Anatytical lietters*.**2016**,*49(2)*,200-207. https://doi: 10.1080/00032719.2015.1067813.
6. Muhammad, F.R.;Umbreen, F.Q. ;Nazar, M.R. ;Imran, M.N. Development and validation of reversed phase high performance liquid chromatography(RP-HPLC) for quanitification of captopril in rabbit plasma. *Acta Chromatographica*.**2020**,*33(4)*,315-321. https://doi:10.1556/1326.2020.00816
7. British pharmacopoeia,London:The stationery office, **2020**:*I424*. https://www.pharmacopoeia.com/downloads/bp/2020/
8. United State Pharmacopoeia and National Formulary USP41 NF36. ,**2018**,*1,677*. https://search.worldcat.org/title/united-states-pharmacopeia-2018-usp-41-the-national-formulary-nf-36/oclc/1013752699 .
9. European pharmacpoeia,Concil of Eruope,France-**2019**, *1,2075*. https://www.sigmaaldrich.com/IQ/en/product/sial/c0430000
10. Nasser, B. ;Khaled, S. ; Zaid, M.E. ;Abdelkrim, C. Chiral analysis of captopril derivatives by HPLC methods. *Acta scientific medical sciences*.**2019**,*3*,187-192. https://www.actascientific.com/ASMS/pdf/ASMS-03-0333.pdf.
11. Nada, A.D.;Roslinda, R.;Harrizul, R. Overview of the determination of captopril levels in pharmaceutical preparations and biological matrices. *Int. Journal of Pharmaceutical Sciences and Medicine(IJPSM)*.**2021**,*6(4)*,1-11. https://doi: 10.47760/ijpsm.2021.v06i04.001.
12. Sigit, M.L.;Rahman, M.A. ; Utamayasa, K.A.: Comparison of the effects of giving captopril and valsartan in cases of heart failure for people with congenital heart disease. *Eur Asian Journal of BioSciences*.**2020**,*14(2)*,3463-3467. https://scholar.google.com/scholar?hl=en&as_sdt=0%2C5&q=Comparison+of+the+effects+of+giving+captopril+and+valsartan+in+cases+of+heart+failure+for+people+with+congenital+heart+disease&btnG=.
13. Eman, S.E.;Hanan, A.M. A liquid chromatography/tandem mass spectrometric method for determination of captopril in human plasma: Application to a bioequivalence study. *Journal of Applied Pharmaceutical Science*.**2017**,*7(2)*,8-15. https://doi:10.7324/JAPS.2017.70202.

14. Razium, A.S.;Mawada, M.T.;Selcan, K. ; Nazar, K. Highly sensitive electrochemical determination of captopril using CuO modified ITO electrod:the effect of in situ grown nanostructures over signal sensitivity. *Royal Society of Chemistry*.**2017**,*7*,19353-19362. https://doi:10.1039/C7RA01538K.
15. Liang, Q.; Wang, Y.; Zheng, M.;Chen, Y.; Huang, W.; Li, G.; Huang, B. Sensitive detection of captopril based on Off-On" carbon dots as fluorescent probe. *Chinese Journal of Luminescence*.**2022**,*43(3)*, 430-439. https://doi:10.37188/CJL.20210372.
16. Liliya, K.S. ;Nataliya, N.Z. Automated quantitation of captopril in pharmaceutical preparations using flow-injection spectrophotometry. *J. Flow Injection Anal*.**2019**,*36(1)*,33-38. https://www.jstage.jst.go.jp/article/jfia/36/1/36_33/_pdf.
17. Dashne, M.K.;Tara, F.T.;Kurdistan, F.A. Spectrophotometric indirect determination of captopril through redox reaction with n-bromosuccinimide and RB dye in pharmaceutical products. *The scientific journal of Koya university*.**2020**,*8(2)*,8-14. https://doi:10.14500/aro.10662.
18. Ratna, B.P.;Olivia, D.;Yunda, D.A.;Endang, L.;Angi, N.B. Validation of high-performance liquid chromatographic method for assay and dissolution of captopril in mucoadhesive tablet formulation. *Journal of Applied Pharmaceutical Science*.**2021**,*11(02)*, 066-074. https://doi:10.7324/JAPS.2021.110209.
19. Changqinng,T.; Xinrong,W. Spectrophotometric determination of captopril in pharmaceutical sample by phosphomolybidc blue. *International Conference on Civil,Architecture and Disaster Prevention*.**2018**:1-5. https://doi:10.1088/1755-1315/218/1/012141.
20. Borhade, A.S. ;Patel, S. ;Chordiya, B.D.;Dalvi, A.M.;Alhat, V. Area under curve UV spectrophotometric method for determination of captopril in bulk and chromatographic method development for the identification of captopril by TLC. *American Journal of PharmtechResearch*.**2019**,*9(03)*,133-140. https://doi:10.46624/ajptr.2019.v9.i3.009.
21. Asmaa, G.D.;Nagham, N.H.;Lazeeza, S.O. H-point srandard addition method for the simultaneous spectrophotometric determination of captopril and hydrochlorothiazide in pharmaceutical formulations. *Jordan Journal of Chemistry*.**2021**,*16(2)*,77-85. https://doi:10.47014/16.2.4.
22. Noor, H. D.; Nashwan, H. A. Spectrophotometric determination of captopril in pharmaceutical formulations based on ion-pair reaction with the red congo. *Journal of Pharmaceutical Negative Results*. 2022; 13(7): 36-42. https://doi:10.47750/pnr.2022.13.S07.006.
23. Yousif, T.M. ; Shirwan, O.B. New batch and flow injection spectrophotometric method for determination of captopril in some pharmaceutical products. *Polytechnic journal*.**2018**,*8(2)*,207-221 . https://www.researchgate.net/publication/326710844.
24. Erlando, S.J. ;Wanessa, R.M. ;Fa'bio, R.P.R. Flow-Injection iodimetric determination of captopril in pharmaceutical preparations. *J. Braz. Chem. Soc*. **2009**,*20(2)*,236-242. https://doi:10.1590/S0103-50532009000200007.
25. Fernando, C.V.; Willian, T.S.; E'der, T.G.; Orlando, F. Flow-Injection spectrophotometric determination of captopril in pharmaceutical formulations using a new solid-phase reactor containing AgSCN immobilized in a polyurethane resin. *Brazilian Journal of Pharmaceutical Sciences*. **2012**, *48(2)*,325-333. https://doi:10.1590/S1984-82502012000200016.
26. Mariam, E.P. ;Beatriz, S.F. Flow injection biamperometric determination of captopril. *Journal of Pharmaceutical and Biomedical Analysis*.**2002**,*30*,547-552.https://doi:10.1016/S0731-7085(02)00315-1.

27. Anastasios, E. ; Demetrius, G.T. ; Georgios, T. ;Paraskevas, D.T. Sensitive determination of captopril by flow injection analysis with chemiluminescence detection based on the enhancement of the luminol reaction .*Analytical Cheimica Acta*. **2002**,*463*,249-255. https://doi:10.1016/S0003-2670(02)00424-5.
28. Willian, T.S. ;Alexandro, A.M ;Luiz, C.S.; Figueiredo, F. ;Orlando, F. Flow injection spectrophotometric system for captopril determination in pharmaceuticals. *J.Braz. Chem. Soc*. **2007**, *18(6)*,1215-1219. https://doi:10.1590/S0103-50532007000600016.
29. Veerubhotla, K.;Walker, R.B. Development and validation of stability-indicating RP-HPLC method using quality by design for estimating captopril. *Indian Journal of Pharmaceutical Sciences*.**2019**,*81(1)*,45-56. https://doi:10.4172/pharmaceutical-sciences.1000478.
30. Cem, E.; Bengi, U. Green procedure index assessment of the nove stability-indicating RP-HPLC method for the determination of captopril from pharmaceutical dosage form. *J. Fac. Pharm. Ankara*.2023; *47(3):* 894-906. https://doi:10.33483/jfpau.1319958.
31. Rana, S.A. ;Enass, N.O. A theoretical study for determination of capoten by analytical methods. *Indian Journal of Forensic Medicine& Toxicology*.**2021**;*15(4)*,3464-3474. https://doi:10.37506/ijfmt.v15i4.17728.
32. Marjan, P.; Trajan, B.; Liliya, L. Development and validation of a fast and simple HPLC method for the simultaneous determination of bisoprolol and enalapril in dosage form. *Pharmacia* .2021;*68(1):* 69-77. https://doi:10.3897/pharmacia.68.50919.
33. Erdem, K.; Ebru, Ç. D.; Doğan, D.; Zehra Ü.; İlkay K.; Güleren A. Development and validation of RPLC method for the simultaneous analysis of ACE inhibitors in tablet formulations. *Turkish Journal of Analytical Chemistry*. **2022**; *4(2):* 103-110. https://doi: 10.51435/turkjac.1176649.
34. Jeber, J.N.; Turkey, N.S. A turbidimetric method for the quantitative determination of cyproheptadine hydrochloride in tablets using an optoelectronic detector based on the LEDs array. *International Journal of Pharmaceutical Research*.**2020**,*12(4)*,2911-2924. https://doi:10.31838/ijpr/2020.12.04.401.
35. Nagam, S.T. ; Elham, N.M. Continuous flow injection analysis , turbidmetric and photometric determination of methyldopa using a new long distance chasing photometer (NAG-ADF-300-2).*Indian Journal of Forensic Medicine &Toxicology*.**2020**,*14(4)*,1835-1841. https://doi:10.37506/ijfmt.v14i4.11810.
36. Elham, N.M. ;Nagam, S.T. New method for the evaluation of propranolol with phosphotungstic acidvialong distance chasing photometer (NAG-ADF-300-2) using continuous flow injection analysis. *International Journal of pharmaceutical Research*.**2019**,*11(4)*,41-57. https://doi:10.31838/ijpr/2019.11.04.008.
37. Nagam, S.T. ; Elham, N.M. Assessment of long distance chasing photometer (NAG-ADF-300-2) by estimating the drug atenolol with ammonium molybdate via continuous flow injection analysis . *Baghdad Science Journal*.**2020**,*17(1)*,78-92. https://doi:10.21123/bsj.2020.17.1.0078.
38. Elham, N.M. ; Nagam, S.T. Assessment of long distance chasing photometer (NAG-ADF-300-2) by estimating the drug Atenolol with povidone iodine via CFIA. *Ibn Al Haitham Journal for Pure and Applied Science*. **2020**, *33(1)*,65-83. https://doi:10.30526/33.1.2383.

39. Nagam, S.T. ; Elham, N.M. Simple and rapid method for estimate of propranolol with Bi(III) via Long-Distance chasing photometer (NAG-ADF-300-2) utilization continuous flow injection analysis. *IJDDT*.**2019**,*9(4)*,563-574). https://doi: 10.25258/ijddt.9.4.9.
40. Nagam, S.T. ; Elham, N.M. Newly developed method for determination of methyldopa drug using ammonium ceric(IV)nitrate by continuous flow injection analysis via homemade NAG-ADF-300-2 analyser. *Annals of Tropical Medicine & Public Health*. **2021**,*24(04)*,528-533. https://doi:10.36295/ASRO.2021.24460 .
41. Nagam, S.T.; Kadhim, M.K. Simple flow injection analysis system for theturbidimetric determination of chromium(III) ion with mefenamic acid using Ayah 6Sx1-ST-2D Solar cell CFIA. *International Journal Of Research In Pharmacy And Chemistry*.**2016**, *6(4)*,759-772. https://scholar.google.com/scholar?hl=en&as_sdt=0%2C5&q=+Ayah+6SX1-ST-2D+solar+cell-CFI+analyser&btnG.
42. Nagam, S.T.;Kefah, H.I. New mode for on-line determination of metoclopramide hydrochloride in pure and pharmaceutical preparation via the use of homemade Ayah 6SX1-T-2D solar cell CFI analyser. *Iraqi journal of science*. **2015**,*56(2)*,1533-1552. https://scholar.google.com/citations?view_op=view_citation&hl=ar&user=taq_QRkAAAAJ&citation_for_view=taq_QRkAAAAJ:u5HHmVD_uO8C.
43. Nagam, S.T. ;Kefah, H.I. Turbidimetric determination of metoclopramide hydrochloride in pharmaceutical preparation via the use of a new homemade Ayah 6SX1-T-2D solar cell-continuous flow injection analyser. *Iraqi journal of science*. **2015**,*56(2B)*,1224-1240. https://scholar.google.com/citations?view_op=view_citation&hl=ar&user=taq_QRkAAAAJ&citation_for_view=taq_QRkAAAAJ:9yKSN-GCB0IC .
44. Raed, F.H. New mode semi-automated turbidimetric determination of mefenamic acid by Ayah 6SX1-ST-2D solar cell-CFI analyser. *Research Journal of Pharmacy and Technology*.**2019**,*12(12)*,5773-5780. https://doi: 10.5958/0974-360X.2019.00999.5.
45. Nagam, S.T. ;Mustafa, K.K. Determination of mefenamic acid using Ce(IV) sulfate as an oxidant reagent via the use of a new mode of irradiation(array of six identical leds) and detection (twin solar cells) through turbidity measurement by CFIA. *International journal of research in pharmacy and chemistry*. **2016**,*6(2)*, 271-290 . https://www.ijrpc.com/files/11-04-16/09-646.pdf.
46. Nagam, S.T. ; Mustafa, K.K. Determination of mfenamic acid using a new mode of irradiation (Ayah of six identical leds) and detection (twin solar cells) through turbidity measurement by CFIA. *Iraqi journal of science*. **2016**,*57(23)*,1052-1070. https://ijs.uobaghdad.edu.iq/index.php/eijs/article/view/7249.
47. Nagam, S.T. ; Rana, A.K. CFIA turbidimetric and photometric determination of vitamin B_9 (Folic acid) using leds as a source of irradiation and two solar cell as an energy transducer .*Baghdad science journal*.**2017**,*14(4)*,773-786 . https://doi:10.21123/bsj.2017.14.4.0773.
48. Nief, R.A. Indirect spectrophotometric determination of captopril in pharmaceutical tablets and spiked environmental samples. *Iraqi National Journal Chemistry*.**2013**, *49*,1-11 https://injchemistry.uobabylon.edu.iq/index.php/chem/article/view/196.
49. Miler ,J.C. ; Miler,J.N.. *Statistics for analytical chemistry* .6th ed. **2010**, St. John Wiley and N.Y.Sons. https://www.africanfoodsafetynetwork.org/wp-content/uploads/2021/09/Statistics-and-Chemometrics-2010.pdf.
50. Murdoch J. ; Barnes J.A. *Statistical tabltes*.4th ed. **1998**, Macmillan. https://scmathuitmkedah.github.io/STA404/files/Full%20Table%20STA404.pdf.